Endothelial Jag1-RBPJ signalling promotes inflammatory leukocyte recruitment and atherosclerosis

Running title: Endothelial Notch signalling promotes atherosclerosis

Meritxell Nus[1,2†]; Beatriz Martínez-Poveda[1†]; Donal MacGrogan[1†]; Rafael Chevre[3]; Gaetano D`Amato[1]; Mauro Sbroggio[1]; Cristina Rodríguez[4]; José Martínez-González[4]; Vicente Andrés[3]; Andrés Hidalgo[5,6]; José Luis de la Pompa[1*]

[1]Intercellular Signalling in Cardiovascular Development & Disease Laboratory, Centro Nacional de Investigaciones Cardiovasculares Carlos III (CNIC), Melchor Fernández Almagro 3, 28029 Madrid, SPAIN; [2] Division of Cardiovascular Medicine, Department of Medicine, University of Cambridge, United Kingdom; [3]Molecular and Genetic Cardiovascular Pathophysiology Laboratory, CNIC; [4] Centro de Investigación Cardiovascular (CSIC-ICCC), IIB Sant Pau. Sant Antoni María Claret 167, 08025 Barcelona, SPAIN; [5]Imaging Cardiovascular Inflammation and the Immune Response Laboratory, CNIC; and [6]Institute for Cardiovascular Prevention, Ludwig-Maximilians University, Munich, Germany

[†] M.N., B.M.P. and D. M. contributed equally to this paper.

* Corresponding author: José Luis de la Pompa, Tel: +34-620-936633. Fax: +34-91-4531240, Email: jlpompa@cnic.es

Phone: +34-620-936633. Fax: +34-91-4531240

Figures: 7 (+Supplemental Material: *Online Methods* section, *Figures S1-S6, Table S1*, *Table S2* and *Table S3* plus two *Online Movies*)

ABSTRACT

Aim: To determine the role of NOTCH during the arterial injury response and the subsequent chronic arterial-wall inflammation underlying atherosclerosis.

Methods and results: We have generated a mouse model of endothelial-specific (*Cdh5*-driven) depletion of the Notch effector RBPJ (*ApoE*$^{-/-}$;*RBPJ*$^{flox/flox}$;*Cdh5-Cre*^{ERT}). Endothelial-specific deletion of *RBPJ* or systemic deletion of *Notch1* in athero-susceptible *ApoE*$^{-/-}$ mice fed a high cholesterol diet for 6 weeks resulted in reduced atherosclerosis in the aortic arch and sinus. Intravital microscopy revealed decreased leukocyte rolling on the endothelium of *ApoE*$^{-/-}$;*RBPJ*$^{flox/flox}$;*Cdh5-Cre*^{ERT} mice, correlating with a lowered content of leukocytes and macrophages in the vascular wall. Transcriptome analysis revealed downregulation of proinflammatory and endothelial activation pathways in atherosclerotic tissue of *RBPJ*-mutant mice. During normal Notch activation, Jagged1 signalling upregulation in endothelial cells promotes nuclear translocation of the Notch1 intracellular domain (N1ICD) and its physical interaction with NF-κB. This N1ICD–NF-κB interaction is required for reciprocal transactivation of target genes, including *vascular cell adhesion molecule-1* (*Vcam1*).

Conclusions: Notch signalling pathway inactivation decreases leukocyte rolling, thereby preventing endothelial dysfunction and vascular inflammation. Attenuation of Notch signalling might provide a treatment strategy for atherosclerosis.

Key words: atherosclerosis; endothelium; inflammation; Notch; NF-κB; transcriptional regulation

Nonstandard Abbreviations and Acronyms

ApoE Apolipoprotein E

BAEC Bovine Aortic Endothelial Cell

CAD coronary artery disease

Cdh5-Cre^{ERT} *Cadherin 5-Cre^{ERT}*, tamoxifen inducible driver mice

DAPT γ -secretase/Notch signalling pathway inhibitor N-[N-(3,5-Difluorophenacetyl)-L-alanyl]-S-phenylglycine t-butyl ester

DMSO dimethyl sulfoxide

HCD High cholesterol diet

HUVEC Human Umbilical Vein Endothelial Cells

Ikbka Inhibitor of Kappa Light Polypeptide Gene Enhancer in B Cells

NECD Notch extracellular domain

NF-κB Nuclear factor-κ B

NICD Notch intracellular domain

Notch1$^{+/-}$ Heterozygous *Notch1* mutant mice

PAEC Porcine Aortic Endothelial Cells

RBPJ recombination signal binding protein for immunoglobulin kappa J region

RBPJ$^{+/-}$ Heterozygous *RBPJ* mutant mice

RBPJ$^{flox/flox}$ Homozygous *RBPJk* conditional mice

RO γ -secretase/Notch signalling pathway inhibitor RO4929097

TNFα Tumor necrosis factor alpha

Introduction

The endothelium plays a central role in vascular physiology, and endothelial dysfunction is intimately associated with vascular disease [1-3]. Endothelial dysfunction is often preceded by "activation", characterized by the induction of proinflammatory signalling cascades and increased expression of vascular adhesion molecules on the endothelial cell surface. These events stimulate the recruitment of leukocytes to the arterial wall and the initiation of the inflammatory and immune processes that promote atheroma initiation and progression in humans and mice. [4-6]

Notch is a highly conserved intercellular signalling pathway that regulates many aspects of organismal development and postnatal tissue homeostasis [7]. Notch receptors (Notch 1-4), are expressed at the cell surface as heterodimers consisting of an extracellular region (NECD) and a membrane-tethered intracellular domain (NICD). The NECD interacts with membrane-bound ligands of the Delta-like (Dll1, Dll3, and Dll4) and Jagged (Jag 1 and Jag2) families expressed on adjacent cells, triggering a series of cleavages in the NICD. Cleavage by the γ-secretase complex releases NICD, which is then translocated to the nucleus [8]. In the nucleus, the NICD forms a complex with the RBPJ/CSL effector transcription factor, resulting in activation of target genes, including those encoding the Hes and Hey families of transcriptional repressors [9].

Notch pathway elements are expressed broadly in the vascular endothelium and smooth muscle from early developmental stages [10, 11]. Their function is to maintain proper artery, capillary and vein organization [12] and to regulate vascular smooth muscle cell differentiation and the response to vascular injury [11, 13]. Notch pathway elements are activated after experimentally induced vascular injury [14, 15], and blockade of Notch signalling compromises vascular repair and pathological remodeling [1617, 18], underscoring the importance of this pathway in maintaining vascular wall homeostasis.

We found multiple components of the NOTCH pathway to be upregulated in human atherosclerotic lesions and in the hyperlipidemic apolipoprotein E–knockout (*ApoE*$^{-/-}$) mouse model of atherosclerosis, suggesting an important function for NOTCH signalling during the chronic inflammation underlying atherosclerosis. To study the contribution of NOTCH signalling to this process, we combined genetic models of systemic (*RBPJ*$^{+/-}$ and *Notch1*$^{+/-}$) and endothelial-specific (*RBPJ*$^{flox/flox}$*;Cdh5-Cre*$^{ERT/+}$) Notch deficiency with the *ApoE*$^{-/-}$ mouse model. We show that canonical Notch deficiency in the

endothelium of cholesterol-fed *ApoE*$^{-/-}$ mice decreases atherosclerosis, secretion of inflammation-related factors, and leukocyte recruitment to the arterial wall. Transcriptome analysis indicates that endothelial Notch-RBPJ signalling favours disease progression during atherosclerosis through a process largely driven by NF-κB-mediated inflammation. We also show that N1ICD binds to both IKK α and NF-kB-p65, and that its interaction with NF-kB-p65 is enhanced by proinflammatory signals and promotes nuclear localization in endothelial cells. We propose that synergy between Notch and NF-kB signalling in the endothelium ensures an adequate inflammatory response by promoting robust and sustained bi-directional target gene transactivation. Given the strong activation of NOTCH signalling in atherosclerotic coronary arteries of CAD patients, attenuating NOTCH signalling in the endothelium represents a potential therapeutic strategy for CAD.

Material and Methods

Materials and Methods are available in the online Data Supplement.

Results

Enhanced expression of Notch pathway components in human and mouse atherosclerotic lesions

To explore the clinical relevance of the Notch pathway during atherosclerosis we examined the expression of NOTCH pathway components in human atherosclerotic coronary arteries. Western blot analysis revealed markedly increased protein levels of NOTCH1 (full-length and cleaved), JAG1, and HES1 in atherosclerotic coronary arteries from coronary artery disease (CAD) patients (*Figure 1A*). qRT-PCR analysis revealed corresponding increases in *NOTCH1*, *JAG1* and *HES1* mRNA expression (*Figure 1B*). These data highlight the clinical importance of Notch signalling activation in CAD.

Similar results were obtained upon examination of aortic-root cross-sections from C57BL/6 control mice and *ApoE*$^{-/-}$ mice fed a high-cholesterol diet (HCD) for 6 weeks. Thus, Jagged1, Notch1, NICD and Hes1 were all upregulated in the endothelium of *ApoE*$^{-/-}$ mice at atherosclerotic and non-atherosclerotic plaque sites (*Figure 1, C-F*). The expression of Dll4, *Notch2*, *Notch4* and *Hey1* was increased although more readily within cells located inside the atherosclerotic plaque (Supplementary material online, *Figure S1A-D*). Exposing mouse *ApoE*$^{-/-}$ aortic endothelial cells (MAEC) to the pro-inflammatory cytokine TNFα

strongly upregulated the expression of *Notch1-4*, *Jag1*, *Hes1*, *Hey1* and *Hey2* mRNA, but not Dll4 (Supplementary material online, *Figure S1E*). Western blot confirmed TNFα-induced increases in Jag1 and Hes1 protein expression (Supplementary material online, *Figure S1F*). Oxidation of low-density lipoproteins (LDL) is a primary factor triggering atherogenesis [19]. To examine the effect of ox-LDL in vitro, MAECs were exposed to a sub-apoptotic concentration of ox-LDL (25μg/mL) for 24h. This treatment resulted in a sharp increase of *Notch1-4*, *Jag1, Dll4, Hes1* and *Hey2* mRNA, but not *Hey1* (Supplementary material online, *Figure S1G*). Thus the expression of several Notch pathway genes in MAEC is upregulated by pro-inflammatory/pro-atherogenic factors TNFa and ox-LDL, mimicking the effect of the HCD.

Inactivation of endothelial Notch slows atherosclerosis progression in *ApoE*$^{-/-}$ mice

To determine canonical Notch function in atherosclerosis we crossed mice heterozygous for a targeted mutation in the Notch pathway effector RBJK (*RBPJ*$^{+/-}$) [20] with atherosclerosis-prone *ApoE*$^{-/-}$ mice. [21] Eight-week-old *ApoE*$^{-/-}$;*RBPJ*$^{+/-}$ mice and *ApoE*$^{-/-}$;*RBPJ*$^{+/+}$ control littermates were fed a HCD for 16 weeks and examined for the presence of atherosclerotic lesions. *En face* analysis of Oil-Red O-stained aortas showed a 33% smaller average atheroma plaque area in *ApoE*$^{-/-}$;*RBPJ*$^{+/-}$ mice compared with controls (*Figure 2A,D*) independently of plasma cholesterol levels (Supplementary material online, *Figure S2A-C*), suggesting that Notch-RBPJ signalling is required for atherosclerotic plaque formation. To determine the implication of the Notch1 receptor in this effect, we generated *ApoE*$^{-/-}$;*Notch1*$^{+/-}$ and *ApoE*$^{-/-}$;*Notch1*$^{+/+}$ control littermates and fed them the HCD. *En face* analysis of Oil-Red O-stained aorta revealed an average 2-fold-smaller plaque area in *ApoE*$^{-/-}$;*Notch1*$^{+/-}$ mice compared with *ApoE*$^{-/-}$;*Notch1*$^{+/+}$ control littermates (P<0.05; *Figure 2B,D*), suggesting that Notch1 is indeed responsible, at least in part, for the pro-atherogenic effect of Notch signalling.

To establish if atheroma formation depends on Notch function in the endothelium, we crossed the inducible endothelial-specific Cre driver line *Cdh5-Cre*^{ERT} [22] with floxed *RBPJ* mice [23] in the *ApoE*$^{-/-}$ background. Eight-week-old *ApoE*$^{-/-}$;*RBPJ*$^{flox/flox}$;*Cdh5-Cre*^{ERT} and control *ApoE*$^{-/-}$;*RBPJ*$^{flox/flox}$ littermates were administered 4-hydroxytamoxifen (4-OHT) for 5 consecutive days to induce *RBPJ* recombination and were subsequently fed the HCD. Abrogation of Notch signalling in the aortic endothelium of

ApoE$^{-/-}$;*RBPJ*$^{flox/flox}$;*Cdh5-Cre*^{ERT} mice was verified by downregulated expression of Notch pathway elements (Supplementary material online, *Figure S3*). *In situ hybridization* (ISH) revealed markedly lowered mRNA expression of endothelial *Notch1* and *Hey2* (Supplementary material online, *Figure S3B,E*) and endothelial immunoreactivity for Jag1, N1ICD and Hes1 was also strongly diminished in aortic sections of *ApoE*$^{-/-}$;*RBPJ*$^{flox/flox}$;*Cdh5-Cre*^{ERT} mice (Supplementary material online, *Figure S3A,C,D*).

En face analysis of Oil-Red O-stained aorta revealed an average 3-fold smaller plaque area in *ApoE*$^{-/-}$;*RBPJ*$^{flox/flox}$;*Cdh5- Cre*^{ERT}mice compared with *ApoE*$^{-/-}$;*RBPJ*$^{flox/flox}$ control littermates (P<0.01; *Figure 2C,D*), despite similar serum lipoprotein profiles (Supplementary material online, *Figure S2D-F*), Movat's pentachrome staining of aortic root cross sections confirmed a marked reduction in atheroma plaque formation in *ApoE*$^{-/-}$;*RBPJ*$^{flox/flox}$;*Cdh5-Cre*^{ERT} mice with respect to controls (P<0.01; *Figure 2D,E*).

To quantify disease progression, atherosclerotic lesions were grouped into 3 categories of increasing severity, as previously described [24, 25]. *ApoE*$^{-/-}$;*RBPJ*$^{flox/flox}$;*Cdh5-Cre*^{ERT} mice presented a higher proportion of early plaques (48%) and relatively few advanced plaques (15%). Conversely, *ApoE*$^{-/-}$;*RBPJ*$^{flox/flox}$ control mice had a higher proportion of advanced plaques (72%) and a lower proportion of early plaques (10%) (*Figure 2F*), suggesting that endothelial Notch deletion slows atherosclerosis progression. Consistent with this finding, the most advanced plaques in *ApoE*$^{-/-}$;*RBPJ*$^{flox/flox}$;*Cdh5- Cre*^{ERT} mice contained fewer apoptotic cells than their counterparts in *ApoE*$^{-/-}$;*RBPJ*$^{flox/flox}$ mice, as assessed by TUNEL assay (*Figure 2G,J*).

Endothelial Notch inactivation impairs leukocyte rolling and homing and vascular adhesion molecule expression

To investigate the effect of Notch on myeloid cell recruitment we monitored leukocyte adhesion and immune-cell composition in plaques. Atherosclerotic lesions of *ApoE*$^{-/-}$;*RBPJ*$^{flox/flox}$;*Cdh5-Cre*^{ERT} mice had a below-control macrophage content (P<0.05; *Figure 2H-J* and Supplementary material online, *Figure S4A,B*) but a normal $CD3^+$ T cell content (Supplementary material online, *Figure S4C,D*). Flow cytometry analysis of the whole aorta revealed a decrease of $Gr1^-CD115^+$ monocytes (P=0.036) in *ApoE*$^{-/-}$

;*RBPJ*$^{flox/flox}$;*Cdh5-Cre*^{ERT} mice with respect to their WT *ApoE*$^{-/-}$;*RBPJ*$^{flox/flox}$ counterparts (Supplementary material online, *Figure S4E*). However with regard to the total number of circulating cells, the total number of circulating T cells ($CD3^+$), B cells ($CD45R^+$), patrolling monocytes (Gr^-CD115^+), inflammatory monocytes (Gr^+CD115^+) and neutrophils (Gr^+ $CD115^-$) were similar in *ApoE*$^{-/-}$;*RBPJ*$^{flox/flox}$;*Cdh5-Cre*^{ERT} and *ApoE*$^{-/-}$;*RBPJ*$^{flox/flox}$ mice (Supplementary material online, *Figure S4F*). Moreover, the proportion of Lin^- $ckit^+$ $sca1^+$ bone marrow hematopoietic stem cells was also relatively similar in both groups (Supplementary material online, *Figure S4G*). These data suggest that the paucity of macrophages in the plaques of *ApoE*$^{-/-}$;*RBPJ*$^{flox/flox}$;*Cdh5-Cre*^{ERT} mice is due to reduced leucocyte recruitment rather than impaired production of circulating cells.

To examine the role of endothelial Notch signalling in leukocyte rolling, we grafted BM from *ApoE*$^{-/-}$;*Mafia* transgenic mice into *ApoE*$^{-/-}$;*RBPJ*$^{flox/flox}$;*Cdh5-Cre*^{ERT} mice and *ApoE*$^{-/-}$;*RBPJ*$^{flox/flox}$ littermates, to allow easy identification of GFP-positive circulating monocytes and neutrophils [26]. After total reconstitution, mice were fed a HCD for 3 weeks, and the carotid arteries were examined by intravital microscopy (*Figure 3A*). Leukocyte rolling flux was decreased in *ApoE-/-;RBPJ*$^{flox/flox}$;*Cdh5-Cre*^{ERT} mice compared with control *ApoE*$^{-/-}$;*RBPJ*$^{flox/flox}$ littermates, whereas rolling velocity was faster (Figure 3B,C and Supplementary material online, *Online Movies 1* and *2*). Consistent with reduced leukocyte rolling, there was reduced GFP immunostaining in the aortic-roots of *ApoE*$^{-/-}$;*RBPJ*$^{flox/flox}$;*Cdh5-Cre*^{ERT} mice (*Figure 3D* and *E*).

Leukocyte homing was examined by injecting nucleated BM cells from *ApoE*$^{-/-}$;*Mafia* mice into HC-fed *ApoE*$^{-/-}$;*RBPJ*$^{flox/flox}$;*Cdh5-Cre*^{ERT} mice and control littermates. Aortic-arch *GFP* mRNA expression after 24 hours was lower in *ApoE*$^{-/-}$;*RBPJ*$^{flox/flox}$;*Cdh5-Cre*^{ERT} mice than in controls (*Figure 3F*), reflecting lower recruitment of GFP^+ myeloid leukocytes. To determine the mechanism underlying the reduced rolling and migration, we incubated BCEF-AM-labelled leukocytes (see *Online Suppl. Material*) with TNFα-stimulated MAEC derived from *ApoE*$^{-/-}$;*RBPJ*$^{flox/flox}$;*Cdh5-Cre*^{ERT} mice or littermate controls; fewer leukocytes adhered to the *RBPJ*-deleted MAEC than to controls (*Figure 3G*). Moreover, the impaired leukocyte adhesion correlated with low *Icam1* and *Vcam1* expression in TNFα-stimulated MAEC (*Figure 3H*). Consistent with these data, treatment with the γ-secretase inhibitor DAPT [27] decreased leukocyte adhesion to bovine aortic endothelial cells (BAEC) (*Figure 3I*) and reduced *Icam1*

and *Vcam1* transcription (*Figure 3J*). Taken together, our data suggest that Notch signalling in the endothelium promotes myeloid leukocyte recruitment by sustaining the expression of *Icam1* and *Vcam1*.

Endothelial *RBPJ* ablation attenuates the atherogenic inflammatory programme

To investigate the effector pathways of the Notch-dependent inflammatory response in atherosclerosis, we compared mRNA expression in aortic arches of *ApoE*$^{-/-}$;*RBPJ*$^{flox/flox}$;*Cdh5-Cre*^{ERT} and *ApoE*$^{-/-}$;*RBPJ*$^{flox/flox}$ mice by RNA sequencing (RNA-seq). This study identified a total of 1922 differentially expressed genes (P<0.05), of which 1209 were upregulated in of *ApoE*$^{-/-}$;*RBPJ*$^{flox/flox}$;*Cdh5-Cre*^{ERT} mice and 713 downregulated (Supplementary material online, *Table S1*).

Ingenuity Pathway Analysis (IPA) identified multiple functions and pathways altered in *ApoE*$^{-/-}$;*RBPJ*$^{flox/flox}$;*Cdh5-Cre*^{ERT} mice (*Figure 4* and Supplementary material online, *Table S2*). A selection of 81 differentially expressed transcripts associated to six biological functions defined by Gene Ontology (GO) are shown in *Figure 4A*. Many upregulated genes were associated with cell-to-cell interactions and survival, such as those encoding tight junction or gap-junction proteins like *Tjp1*, *Cldn25* and *Gjc1* and the survival genes *Rictor*, *Akt3* and *Bcl2*, perhaps reflecting changes of vascular permeability. To examine endothelial barrier function in *ApoE*$^{-/-}$;*RBPJ*$^{flox/flox}$;*Cdh5-Cre*^{ERT} mice, we performed Evans blue vascular permeability assay (Supplementary material online, *Figure S5*). We found no significant difference in Evans blue staining or dye content in *ApoE*$^{-/-}$;*RBPJ*$^{flox/flox}$;*Cdh5-Cre*^{ERT} with respect to *ApoE*$^{-/-}$;*RBPJ*$^{flox/flox}$ mice (Supplementary material online, *Figure S5A,B*), suggesting that endothelial barrier function was not impaired.

In contrast, there was a severe downregulation of genes implicated in cellular processes related to inflammation (*Figure 4A*), notably those required for leukocyte-endothelium interaction and leukocyte extravasation. Thus chemokine receptors (*Cxcr2*), cellular mediators of monocyte/macrophage activation like *Ccl2 (MCP1), Ccl7, Ccl12, Ccl4, Cxcl1* and *Ccl3* (*Figure 4A*) and leukocyte adhesion proteins like P-Selectin *(Selp)* and E-Selectin *(Sele)* were sharply decreased. These latter factors are expressed on activated endothelial cells shortly after cytokine activation by tissue macrophages. Other genes involved in immune cell movement and trafficking, such as integrin ligands *Vcam1* and *Icam1* were also downregulated (*Figure 4A*), consistent with our prior *in vitro* observations (*Figure 3H and J*).

Attenuation of the global inflammatory response was further evidenced by decreased expression of classical mediators of immunity, including interleukins and their corresponding receptors (*Il1b/Il1r2*, *Il6/Il6r*, *Tnf/Tnfrsf1b)*. Importantly, the aortic arch of *ApoE*$^{-/-}$*;RBPJ*$^{flox/flox}$*;Cdh5-Cre*^{ERT} mice showed significant downregulation of members of pathways previously associated with atherosclerosis, such as prototypical components of the NF-kB signalling pathway (*RelB, Nfkbie, Nfkbid, Nfkb2* and *Nfkbia*), matrix metalloproteases (including *Mmp2* and *Mmp14*, and *Timp1*), and Toll-like receptors pathways (*Tlr1*, *Tlr2* and *Tlr6*; *Figure 4A*). Interestingly, among the upregulated genes important for the inflammatory response, *Tgfβ3* and its receptor Tgfb3r were reported previously in relation to atherosclerosis development in *ApoE*$^{-/-}$ mice [28]. These findings were confirmed by canonical pathways analysis (Supplementary material online, *Table S2*). For example, the NF-kB, IL6, acute phase inflammatory response, and Toll-like receptor pathways were all significantly downregulated, whereas *Tgfβ* was upregulated (*Figure 4B*). Changes in the expression of several key genes implicated in endothelial activation and inflammation were validated by qRT-PCR (*Figure 4C*) and/or immunohistochemistry (*Figure 4D-F*).

The RNA-seq also detected differential modulation of genes associated with cellular growth and proliferation; for example, the cell-cycle inhibitor CDKN1A (p21) was downregulated, whereas CDKN1B (p27) was upregulated (*Figure 4A* and Supplementary material online, *Table S1*), consistent with CDKN1A being atherogenic and CDKN1B atheroprotective [29]. Nevertheless, proliferation measured by Ki67 staining in plaques from *ApoE*$^{-/-}$*;RBPJ*$^{flox/flox}$*;Cdh5-Cre*^{ERT} mice was not significantly different from control (Supplementary material online, *Figure S5C,D*). Taken together, the RNA-seq data analysis indicates that endothelial-specific Notch ablation suppresses the proinflammatory genetic programme associated with atherosclerosis.

Notch interacts with NF-kB in endothelial cells and facilitates NF-kB nuclear localization

Many of the putative RBPJ target genes identified by RNA-seq are also targets for NF-kB (nuclear factor kappa B; http://bioinfo.lifl.fr/NF-KB/). NF-kB is a family of transcription factors whose predominant form, p65/p50, is maintained in an inactive state in the cytoplasm through interaction with Ikbka [30]. In response to inflammatory stimuli elicited by cytokines such as TNFα, Ikbka is phosphorylated by the

IKK complex and releases p65/p50, which translocates to the nucleus and activates transcription of genes containing kB sites in their promoter [30]. Given that endothelial NF-kB signalling activation is critical for inflammation and atherogenesis in mice [24], we hypothesized that Notch might act upstream of, or in parallel with, NF-kB to regulate common target genes.

Studies in different cellular systems have determined that the physical interaction between N1ICD and NF-kB facilitates NF-kB nuclear translocation and/or retention [31-36]. To determine if N1ICD promotes NF-kB nuclear translocation in endothelial cells, we monitored the levels of nuclear and cytoplasmic NF-kB-p65 protein over time in response to TNFα. After 30 min in the presence of TNFα the proportion of nuclear NF-kB-p65 staining was markedly reduced (P<0.01) in *ApoE*$^{-/-}$*;RBPJ*$^{flox/flox}$*;Cdh5-Cre*^{ERT} MAEC compared to *ApoE*$^{-/-}$*;RBPJ*$^{flox/flox}$ MAEC (*Figure 5A,B*), whereas the proportion of nuclear and cytoplasmic staining was higher (P<0.05), suggesting that p65 nuclear translocation is blocked or delayed in MAEC lacking *RBPJk*. In addition, analysis of nucleo-cytoplasmic fractions by Western blot indicated that TNFα-stimulated NF-kB-p65 nuclear accumulation after 30 min was 2.5-fold increased in *ApoE*$^{-/-}$*;RBPJ*$^{flox/flox}$ MAEC compared to 2-fold in *ApoE*$^{-/-}$*;RBPJ*$^{flox/flox}$*;Cdh5-Cre*^{ERT} MAEC (*Figure 5C,D*). Delayed TNFα-induced p65 nuclear entry was also observed after treating human umbilical vein endothelial cells (HUVEC) with the γ-secretase inhibitor RO4929097 [37] (Supplementary material online, *Figure S6A-D*).

N1ICD is known to facilitate NF-kB nuclear translocation in cancer cells and valve aortic interstitial cells by interacting with the IKK complex [34-36]. To determine if N1ICD-IKKα interaction increases the nuclear presence of NF-kB-p65 in endothelial cells, we immunoprecipitated N1ICD from porcine aortic endothelial cells (PAEC) overexpressing a myc-tagged version of N1ICD [27]. IKKα and N1ICD were co-immunoprecipitated from untreated PAEC N1ICD cells, and this interaction was enhanced by treatment with TNFα (*Figure 5D*). Myc-tagged N1ICD from PAEC also co-immunoprecipated NF-kB-p65/p50 (*Figure 5E*), and TNFα stimulation also increased N1ICD binding to NF-kB-p65 and the amount of immunoprecipated NF-kB in HUVEC (*Figure 5F*). Taken together, these results indicate that N1ICD can bind to both IKKα and NF-kB-p65. Its interaction with NF-kB-p65 is enhanced by proinflammatory signals and promotes NF-kB nuclear localization in endothelial cells.

N1ICD and NF-kB coactivate the inflammatory response in endothelial cells

An anticipated functional outcome of increased nuclear NF-kB-N1ICD complex formation is that the transactivation of target genes common to both NFkB and N1ICD is more sustained or prolonged. Treating HUVEC with TNFα resulted in marked induction of *VCAM-1*, *ICAM-1*, *SELE* and *NFKB2* and *NFkBIα* expression (*Figure 6A*). This effect was almost completely abolished by pre-treating cells with the chemical NF-kB inhibitor BAY-11-7082 (BAY-11) (*Figure 6A*). TNFα also increased the expression of *JAG1* and *HEY1*, and this effect was blocked by BAY-11 (*Figure 6A*), suggesting that the expression of TNFα-induced Notch-pathway genes is dependent on NF-kB activation. These results were confirmed by western analysis of JAG1 and VCAM1 (*Figure 6B*). BAY-11 only partially reduced JAG1 levels, suggesting that JAG1 protein levels depend on additional factors (*Figure 6B*). These data suggest NF-kB activation is required for the TNFα-mediated stimulation of target gene transcription by both NF-kB and NOTCH pathways.

We next examined the effect of *RBPJ* genetic disruption upon TNFα stimulation in MAEC. In *ApoE*$^{-/-}$ MAEC, TNFα sustains the mRNA and protein expression of Notch pathway components (*Notch1*, *Notch2, Notch4, Jag1*, *Dll4*, *Hes1*, *Hey1* and *Hey2*) and Vcam1, Icam1 (*Figure 3H*) and *Nfkbiα* (*Figure 6C,D*). However this effect was suppressed in *ApoE*$^{-/-}$*;RBPJ*$^{flox/flox}$*;Cdh5-Cre*^{ERT} MAEC, indicating that RBPJ is required for TNFα-induced gene expression in MAEC . Consistent with this, TNFα induction of Notch and NF-kB targets in BAEC was partially blocked by DAPT (Supplementary material online, *Figure S6E,F*). Accordingly, NF-kB luciferase reporter activity increased 3.5-fold in BAEC in response to TNFα, and this effect was reduced to 2-fold by pre-treating with DAPT (*Figure 6E*). These data suggest that Notch activation is required for TNF α -stimulated expression of NF-kB and Notch target genes.

To determine if increased NICD-RBPJ signalling can activate NF-kB independently of TNFα, we cultured HUVEC on plastic dishes coated with the extracellular domain of the NOTCH ligand JAG1. JAG1 ligand stimulation induced the NOTCH target genes *DLL4, JAG1, HES1* and *HEY1* as well as several NF-kB target genes, including *VCAM1, ICAM1, SELE*, *NFKB2* and *NFKBIα* (*Figure 6F*),

indicating that NOTCH activation by JAG1 can lead to the upregulation of NF-kB target genes. To determine whether the effects of JAG1 and TNFα were additive, we cultured HUVEC with TNFα alone or together in presence of immobilized JAG1 extracellular domain. Although *NFKB2* was not affected, a combination of TNFα and JAG1 induced an average 2-fold increase in the activation of the NOTCH and NF-kB target genes *JAG1*, *HEY1*, *ICAM1*, *VCAM1*, *SELE*, and *NFKBIα* compared with the effect of TNFα alone (*Figure 6G*). These results suggest that the effects of TNFα and JAG1 are additive. Taken together, our data indicate that TNFα-stimulated transcription of NF-kB and NOTCH target genes requires the concerted activation of NICD-RBPJ and NF-kB signalling.

Discussion

In this study we addressed the role of canonical (RBPJ-mediated) Notch signalling in the adult endothelium and identified an important and unexpected pro-atherogenic Notch function in atherosclerosis. Thus, endothelial-specific deletion of Notch signalling in *ApoE*$^{-/-}$ mice (*ApoE*$^{-/-}$;*RBPJ*$^{flox/flox}$;*Cdh5-Cre*^{ERT}) causes a marked delay in atherosclerosis progression, a finding confirmed by *in vitro* experiments. Multiple lines of evidence support the notion that endothelial Notch signalling is pro-atherogenic: i) Notch pathway components expression is upregulated in atherosclerotic lesions of CAD patients; ii) endothelial Notch inactivation in *ApoE*$^{-/-}$ mice decreases adhesion molecule expression, leukocyte recruitment, macrophage accumulation and attenuates atheroma plaque severity; iii) endothelial Notch inactivation decreases NFκB-dependent gene expression, impairing the pro-inflammatory response; and iv) Notch signalling promotes the pro-inflammatory/pro-atherogenic response mediated by NFκB both *in vivo* and *in vitro*.

We find, consistent with a prior study [38] that Notch signalling components are upregulated in luminal ECs of human atherosclerotic plaques, supporting a role for this developmental pathway in human CAD. We demonstrate that endothelial Notch inactivation slows the progression of atherosclerosis in *ApoE*$^{-/-}$ mice. Notch signalling activation is required for the inflammatory response elicited in the endothelium, but persistent activation *in vivo* is ultimately detrimental because it results in the chronic inflammatory process underlying atheroma plaque build-up. Previous models of artery injury and studies in endothelial cell cultures have pointed to a protective role of the Notch pathway in atherosclerosis [39, 40]. More recently, Notch pathway gene expression was found to be downregulated in C57/BL6 mice on short-term high fat diet and in human aortic endothelial cells (HAEC) exposed to ox-PAPC or inflammatory cytokines [41]. This effect was linked to increased monocyte binding and diet-induced atherosclerosis in L-sIDOL mice [42] with heterozygous deletion of *Notch1* [41]. These contrasting data may reflect differences in model systems and experimental conditions (short-term versus long-term diets; acute versus chronic inflammation; different origins of the endothelial vascular bed and inter-individual variation) and the complexity of Notch signalling functions, canonical or non-canonical, which are highly context dependent [7].

A pro-atherogenic effect of canonical Notch signalling in the endothelium is supported by the RNA-seq data. We detected significant downregulation of adhesion molecules, remodelling enzymes, and proinflammatory pathways in *ApoE*$^{-/-}$;*RBPJ*$^{flox/flox}$;*Cdh5-Cre*^{ERT} mice, consistent with lower incidence of atherosclerosis and the requirement of endothelial Notch signalling for the inflammatory response. MMPs weaken the arterial wall and contribute to destabilization and rupture of atherosclerotic plaques [43]. Chemokines and their receptors support leukocyte arrest on the endothelium, form chemotactic gradients that promote diapedesis and provide important anti-apoptotic survival cues to leucocytes [44]. Interleukins, their receptors, TNFα pathway components and TLRs are all implicated in the inflammatory response [45]. TLRs recognize pathogens and mediate signalling pathways important for host defense and their effects are not limited to inflammatory cells because they can also alter the behaviour of resident vascular cells [46]. In summary, our RNA-seq data suggest that the inactivation of *RBPJ* in the endothelium negatively impacts key inflammatory processes involved in atherosclerosis progression.

The NF-kB pathway was prominently downregulated after endothelial *RBPJ* deletion. NF-kB is a master regulator of inflammatory responses, both in the initial stages of inflammation and in the resolution phases [47, 48]. Moreover, NF-kB regulates atheroma formation [48, 49] and a signalling mechanism driving atherosclerotic plaque progression in the endothelium [24]. A complex and incompletely understood interplay between Notch and NF-kB has been described in several cell types and contexts, including B cell differentiation, inflammation, injury, and cancer. Depending on the situation, this interplay can lead to either activation or repression of gene transcription [50]. In the context of inflammation, Notch and NF-kB interaction leads ultimately to transcriptional activation. For example, cooperation between Notch and NF-kB in macrophages is essential for the expression of interleukins [51, 52] and inflammatory-associated molecules [53] and for macrophage activation [54-56]. Mechanistically, this synergism has been shown to occur through protein-protein interaction in the cytoplasm that facilitates shuttling to the nucleus [34-36] or through protein-protein interaction in the nucleus that promotes nuclear retention [33]. Moreover, N1ICD binding to NF-kB has been shown to stabilize NF-kB and enhance its binding to target gene promoters [31, 32].

Manipulating Notch and NF-kB activities allowed us to extend many of these findings to endothelial cells by establishing that the nuclear content of NF-kB-p65 is markedly below normal in endothelial cells lacking RBPJ. This implies that RBPJ and NF-kB interact functionally, consistent with

findings in macrophages and other cell systems [31-34, 36, 57]. RBPJ and NF-kB-p60 may interact through N1ICD, since N1ICD can physically bind to NF-kB-p60 (*Figure* 5E,F). Future studies combining ChIP-seq with RNA-seq should shed light on the mechanism of transcriptional co-regulation and identify the full repertoire of genes controlled by Notch and/or NF-kB in endothelial cells. Taken together, our findings support a model of tight integration between the NF-kB and Notch pathways early upon TNFα stimulation, in which N1ICD acts as a transcriptional co-factor of NF-kB and establishes an auto-amplification loop through Jag1 that heightens NF-kB signalling (*Figure 7*). Initially, NF-kB-dependent Jag1 induction in endothelial cells may be mediated by signals emanating from interacting mononuclear cells. Supporting this idea, cell surface expression of Jag1 in c-Rel-expressing cell monolayers functionally interacts with lymphocytes expressing the Notch1 receptor [58-60]. Given that Jag1 expression is widespread in immune cells and tissues [58-60], signalling to Notch1-expressing endothelial cells is also likely. Subsequently, coactivation of Jag1 expression by Notch and NF-kB augments and sustains a subset of NF-kB-inducible genes that are Notch dependent. In a similar fashion, Jag1-mediated cross-amplification between TLR and Notch is required in primary macrophages for the early phases of TLR-induced gene expression and induction of Notch ligands that can modulate later phases of the TLR response [60, 61]. Moreover, feed-forward signalling between Jag1/Notch and NF-kB may constitute a "priming" mechanism that ensures rapid propagation of the inflammatory response from locally athero-susceptible regions to the rest of the endothelium.

The graded pattern of N1ICD expression, between athero-prone *ApoE*$^{-/-}$ and relatively athero-resistent C57/BL6 mice on one hand, and sites of atheroma formation in fat-fed *ApoE*$^{-/-}$ mice on the other (*Figure 1*), suggests that N1ICD expression and disease progression are linked and that a Notch-dependent inflammatory programme precedes overt disease. This possibility could be examined in juvenile *ApoE*$^{-/-}$ mice, which experience low-level inflammation but show no signs of atheroma formation before 4 weeks of age [62]. Early detection of endothelial NOTCH activation may have prognostic value in atherosclerosis, given that endothelial activation and subsequent dysfunction contributes to atherosclerosis severity and progression [2, 63-65]. Moreover, strategies that aim to attenuate NOTCH signalling in the endothelium should be taken into consideration to complement current anti-inflammatory therapies for atherosclerotic vascular disease. Jag1 constitutes a potential early therapeutic target for the

blockade of atherosclerosis and development of coronary artery disease. Immune targeting of Jag1 may provide a potential future strategy for the prevention of atherosclerosis progression either alone or in combination with standard treatments.

Acknowledgments

We thank S. Bartlett (CNIC) for English editing and the CNIC Genomics and Bioinformatics Units for processing sequencing data. M.N., B.M.P., R.C., G.D., M.S. and C.R. performed experiments. M.N., B.M.P. and D.M. analyzed and validated RNA-seq results, J.M.G. provided the samples of atherosclerotic patients, A.H. and V.A. evaluated intravital microscopy data. M.N., B.M.P., D.M. and J.L.d.l.P. evaluated experiments, reviewed the data and wrote the manuscript. All authors reviewed the manuscript.

Sources of Funding

This study was funded by grants SAF2013-45543R, RD12/0042/0005 (RIC) and RD12/0019/0003 (TERCEL) from the Spanish Ministry of Economy and Competitiveness (MINECO) to J.L.dlP, RD12/0042/0028 (RIC) to V.A. and RD12/0042/0053 (RIC) and SAF2012-40127 to J.M.G. M.N. held a Sara Borrell postdoctoral contract (CD09/00452) and D.M. holds a postdoctoral contract associated with grant RD12/0042/0005, both awarded by The Instituto de Salud Carlos III; B.M.P. holds a Juan de la Cierva postdoctoral contract (JCI-2010-06343). The CNIC is supported by the Spanish Ministry of Economy and Competitiveness (MINECO) and the Pro CNIC Foundation, and is a "Severo Ochoa" Center of Excellence (MINECO award SEV-2015-0505).

Disclosures

None

Figure Legends

Figure 1. Notch signalling is upregulated in human and mouse atherosclerosis. (A) Representative western blot showing protein levels of NOTCH1 (full-length and cleaved form or N1ICD), JAG1 and HES1 in atherosclerotic and non-atherosclerotic human coronary arteries. **(B)** Real time-PCR analysis of NOTCH signalling genes in atherosclerotic (n=15) and non-atherosclerotic (n=10) human coronary arteries. Data are means ± SEM. **P*<0.05; ***P*<0.01; ****P*<0.001. **(C-F)** Representative sections of aortic sinus at non-atherosclerotic and atherosclerotic sites in C57/BL6 and *ApoE*$^{-/-}$ mice. **(C)** Jag1 immunohistochemistry (IHC). **(D)** *Notch1 in situ* hybridization (ISH). **(E)** N1ICD immunofluorescence. **(F)** Hes1 IHC. Arrowheads point to endothelial cells and arrows to putative immune cells. Representative of two independent experiments. Scale bars, 50 μ m.

Figure 2. Endothelial deletion of *RBPJ* delays atherosclerosis progression in *ApoE*$^{-/-}$ mice. (A) Representative Oil-red-O *en face* staining of aortas of *ApoE*$^{-/-}$*;RBPJ*$^{+/+}$ and *ApoE*$^{-/-}$*;RBPJ*$^{+/-}$ mice (6-8 weeks-old) fed a HC diet for 4 months. **(B)** Representative Oil-red-O *en face* stainings of aortas of *ApoE*$^{-/-}$*;Notch1*$^{+/+}$ and *ApoE*$^{-/-}$*;Notch1*$^{+/-}$ mice (6-8 weeks-old) fed a HC diet for 6 weeks. **(C)** Representative Oil-red-O *en face* stainings of aortas of *ApoE*$^{-/-}$*;RBPJ*$^{flox/flox}$ and *ApoE*$^{-/-}$*;RBPJ*$^{flox/flox}$*;Cdh5-Cre*^{ERT} mice (6-8 weeks old) induced with 4-hydroxy-tamoxifen on 5 consecutive days and fed a HCD for 6 weeks. (**D**) charts show plaque quantification in aortic arches of *ApoE*$^{-/-}$*;RBPJ*$^{+/+}$ (n=7) and *ApoE*$^{-/-}$*;RBPJ*$^{+/-}$ (n=5) mice; quantification in aortic arches of *ApoE*$^{-/-}$*;Notch1*$^{+/+}$ (n=7) and *ApoE*$^{-/-}$*;Notch1*$^{+/-}$ (n=6) mice; quantification in aortic arches of *ApoE*$^{-/-}$*;RBPJ*$^{flox/flox}$ (n=12) and *ApoE*$^{-/-}$*;RBPJ*$^{flox/flox}$*;Cdh5-Cre*^{ERT} (n=9) mice and quantification of atherosclerotic lesion area in *ApoE*$^{-/-}$*;RBPJ*$^{flox/flox}$ (n=13) and *ApoE*$^{-/-}$*;RBPJ*$^{flox/flox}$*;Cdh5-Cre*^{ERT} (n=22) mice. **(E)** Representative Movat's pentachrome staining of transverse sections of the aortic sinus in *ApoE*$^{-/-}$ and *ApoE*$^{-/-}$*;RBPJ*$^{flox/flox}$*;Cdh5-Cre*^{ERT} mice; scale bars, 50 μ m; chart shows **(F)** Histological staging of atherosclerotic lesions of *ApoE*$^{-/-}$*;RBPJ*$^{flox/flox}$ and *ApoE*$^{-/-}$*;RBPJ*$^{flox/flox}$*;Cdh5-Cre*^{ERT} mice (n=5 per group). The pie chart shows the mean percentage of each type of lesion (early, moderate and advanced) as a percentage of the total atherosclerotic plaque area in each mouse (n=5 mice per genotype). **(G)** Representative TUNEL assay on transverse sections of aortic sinus of *ApoE*$^{-/-}$*;RBPJ*$^{flox/flox}$ and *ApoE*$^{-/-}$*;RBPJ*$^{flox/flox}$*;Cdh5-Cre*^{ERT} mice. Arrowheads point to TUNEL-

positive cells; scale bars, 50μm. **(H,I)** Representative F4/80 immunohistochemistry (brown stain) in transverse sections of aortic sinus of *ApoE$^{-/-}$;RBPJ$^{flox/flox}$* (**H**) and *ApoE$^{-/-}$;RBPJ$^{flox/flox}$;Cdh5-Cre^{ERT}* mice (**I**) and higher magnifications of inset areas. Scale bars, 100μm. **(J)** Quantification of TUNEL positive nuclei (n=4 per group) and of F4/80-positive area in aortic sinus sections of *ApoE$^{-/-}$;RBPJ$^{flox/flox}$* and *ApoE$^{-/-}$;RBPJ$^{flox/flox}$;Cdh5-Cre^{ERT}* mice (n=5 per group). For all the charts, data are means ± SEM. **P*<0.05; ***P*<0.01; ****P*<0.001.

Figure 3. Endothelial deletion of *RBPJ* results in reduced leukocyte recruitment to atheroma-prone regions of the carotid artery. (A) Intravital microscopy image capture of carotid bifurcation in the FITC channel at low magnification. White dashed lines delimit the carotid artery wall. Green dashed lines show areas imaged for the quantification of rolling. White arrow indicates blood flow. Scale bar, 100 μm. **(B)** Quantification of rolling GFP$^+$ myeloid leukocytes in *ApoE$^{-/-}$;RBPJ$^{flox/flox}$* and *ApoE$^{-/-}$;RBPJ$^{flox/flox}$;Cdh5-Cre^{ERT}* mice transplanted with bone marrow from *ApoE$^{-/-}$;Mafia* transgenic mice (GFP$^+$ myeloid leukocytes). Results are normalized to the control group mean (n=15-18 fields from 5 mice/group). Long horizontal lines denote mean values, and error bars denote SEM (each data point denotes a field). **(C)** Quantification of rolling velocity of GFP$^+$ myeloid leukocytes in transplanted *ApoE$^{-/-}$;RBPJ$^{flox/flox}$* and *ApoE$^{-/-}$;RBPJ$^{flox/flox}$;Cdh5-Cre^{ERT}* mice [n=68-82 leukocytes from fields presented in (B)]. **(D)** Representative GFP immunostaining of atherosclerotic plaques in the aortic root of *ApoE$^{-/-}$;RBPJ$^{flox/flox}$; Cdh5-Cre^{ERT}* and *ApoE$^{-/-}$;RBPJ$^{flox/flox}$* mice (n=5 per group) transplanted with BM from *ApoE$^{-/-}$*; *Mafia* transgenic mice and fed a HC diet for 3 weeks. Elastic fibres display autofluorescence. Scale bar, 25μm. **(E)** Numbers of GFP$^+$ cells (neutrophils and macrophages) in atherosclerotic plaques of animals described in (D). **(F)** Relative *GFP* mRNA expression in aortic arches of *ApoE$^{-/-}$;RBPJ$^{flox/flox}$;Cdh5-Cre^{ERT}* mice and *ApoE$^{-/-}$;RBPJ$^{flox/flox}$* littermates (n=5, each group) 24 h after injection with GFP+ nucleated bone marrow cells. **(G)** Quantification of leukocyte adhesion on MAEC derived from *ApoE$^{-/-}$;RBPJ$^{flox/flox}$* and *ApoE$^{-/-}$;RBPJ$^{flox/flox}$;Cdh5-Cre^{ERT}* mice treated with TNF α for 12h. Data represent three biological replicates in two independent experiments. **(H)** Relative expression of *Icam1* and *Vcam1* mRNA in MAEC derived from *ApoE$^{-/-}$;RBPJ$^{flox/flox}$* and *ApoE$^{-/-}$;RBPJ$^{flox/flox}$;Cdh5-Cre^{ERT}* mice treated with TNF α for 24h. Data represent three biological replicates in two independent experiments. **(I)** Quantification of

leukocyte adhesion on BAEC exposed to 10 μM DAPT or vehicle (DMSO) after treatment with TNF α for 24h. Data represent three biological replicates in two independent experiments. **(J)** Relative expression of *Icam1* and *Vcam1* mRNA in BAEC exposed to 10 μM DAPT or vehicle (DMSO) after treatment with TNF α for 24h. Data represent two independent experiments with three biological replicates. For all the charts, data are means ± SEM. **P*<0.05; ***P*<0.01; ****P*<0.001.

Figure 4. Downregulation of proinflammatory gene expression in *ApoE$^{-/-}$;RBPJ$^{flox/flox}$; Cdh5-Cre^{ERT}* mice. (A-C) Global gene expression analysis and validation. **(A)** Circular plot of selected deregulated genes in *ApoE$^{-/-}$;RBPJ$^{flox/flox}$;Cdh5-Cre^{ERT}* mice compared with *ApoE$^{-/-}$;RBPJ$^{flox/flox}$* mice (n=3 per group) identified by RNA-seq. The analysis identified 81 differentially expressed genes belonging to various biological processes relevant to this study. The left semicircle represents differentially regulated genes and the right semicircle represents biological processes. The gene-expression colour scheme represents the logFC for each gene plotted: downregulated in blue and upregulated in red. **(B)** Analysis of canonical pathways for the deregulated genes in *ApoE$^{-/-}$;RBPJ$^{flox/flox}$;Cdh5-Cre^{ERT}* aortic arches. Bars represented - log (B-H P value, Benjamini-Honchberg-adjusted *P value)*. Colour code in bars reflects the direction of change for the function, based on z-score (orange, positive z-score: the pathway is trending towards an increase; blue, negative z-score: the pathway is trending towards a decrease). The ratio indicates the number of differentially expressed genes in a given pathway divided by the total number of genes listed in that pathway. **(C)** Relative mRNA expression of indicated genes measured by qRT-PCR. Data are means ±SEM (n=4-5 aortas per group). **(D-F)** Representative sections of aortic sinus of *ApoE$^{-/-}$;RBPJ$^{flox/flox}$;Cdh5-Cre^{ERT}* and *ApoE$^{-/-}$* mice immunostained for **(D)** Icam1, **(E)** Vcam1 and **(F)** NF-kB-p65. *ApoE$^{-/-}$;RBPJ$^{flox/flox}$;Cdh5-Cre^{ERT}* aortas show lower staining of the luminal endothelial layer (arrowhead). Note that Icam1 and NF-kB immunoreactivity is also detected in immune cells within atherosclerotic plaques (arrow). Representative of two independent experiments. Scale bars, 50 μ m.

Figure 5. N1ICD interacts with NF-kB-p65 (RelA) and is required for its translocation/retention in the nucleus. (A) NF-kB-p65 immunofluorescence in *ApoE$^{-/-}$*; *RBPJ$^{flox/flox}$* and *ApoE$^{-/-}$;RBPJ$^{flox/flox}$;Cdh5-Cre^{ERT}* MAEC without stimulation (t0) and after exposure to TNFα for 30 min . Representative images

of two independent experiments. Scale bar, 30 μm. **(B)** Quantification of cytosolic, cytosolic and nuclear, and nuclear NF-kB p65 staining (ImageJ) in (**A**), **P*<0.05; ***P*<0.01. **(C)** Western blot (WB) detecting nuclear (N), and cytosolic (C) fractions of NF-kB-p65 in *ApoE*$^{-/-}$;*RBPJ*$^{flox/flox}$ and *ApoE*$^{-/-}$;*RBPJ*$^{flox/flox}$;*Cdh5-Cre*^{ERT} MAEC exposed to TNFα at the indicated time points. One of two independent experiments is shown. **(D)** Quantification of western-blot band density (ImageJ). White dots correspond to values determined for different time points shown in (**C**). Black dots correspond to values determined in the replicate Western blot (not shown). **(E)** PAEC were exposed to TNFα for 1 h. (*Top panel*) Immunoprecipitation (IP) with anti-IKKα antibody, WB against N1ICD-Myc. *(Bottom panel)* Whole cell extract (WCE) immunoblot to detect IKKα. One of two independent experiments is shown. **(F)** (*Top panel*) IP with anti-myc antibody, WB with anti-NF-kB-p65. *(Bottom panel)* WCE immunoblot to detect NF-kB-p65. One of two independent experiments is shown. **(G)** (*Top two panels*) HUVEC were exposed to TNF for 1h followed by IP with anti-NF-kB-p65 antibody and WB with anti-N1ICD or anti-NF-kB-p65. (*Bottom two panels*) WCE immunoblots to detect N1ICD or NF-kB-p65. One of two independent experiments is shown.

Figure 6. TNFα-dependent transcription of Notch- and NF-kB-target genes in endothelial cells requires mutual activation of both pathways. (A) qRT-PCR analysis of the relative mRNA expression of indicated genes in HUVEC pretreated with BAY-11 (10μM) or vehicle (DMSO) for 1h and exposed to TNFα for 3h. One of two independent experiments, each with three biological replicates, is shown. **(B)** Immunodetection of JAG1 and VCAM1 proteins in HUVEC pretreated for 1h with BAY-11 (10μM) or DMSO and exposed to TNFα for 8h. One of two independent experiments is shown. (**C**) Relative mRNA expression of indicated genes as detected by qRT-PCR in MAEC exposed to TNFα for 3h. One of two independent experiments, each with three biological replicates, is shown. (**D**) Immunodetection of Jag1, Hes1 and Vcam1 protein in MAEC from *ApoE*$^{-/-}$;*RBPJ*$^{flox/flox}$ and *ApoE*$^{-/-}$;*RBPJ*$^{flox/flox}$;*Cdh5-Cre*^{ERT} mice exposed to TNFα for 8h. One of two independent experiments is shown. (**E**) Activity of the 3XNF-kB-Luciferase reporter construct in BAEC exposed to TNF α for 8 hours in the presence of DAPT or DMSO. Results are representative of three independent experiments, each with six biological replicates. (**F**) qRT-

PCR analysis of relative mRNA expression of the indicated genes in HUVEC plated for 24 hours on JAG1-coated or control plates. Results represent three replicates in two independent experiments. One of two independent experiments, each with three biological replicates, is shown. (**G**) qRT-PCR analysis in HUVEC plated for 24 hours on JAG1-coated plates and exposed to TNFα for 8 hours. One of two independent experiments, each with three biological replicates is shown. For (**A**, **C**, **E**, **F** and **G**), data are means ± SEM. **P*<0.05; ***P*<0.01; ****P*<0.001; n.s., non significant.

Figure 7. Model of Notch and NF-kB signalling crosstalk in the proinflammatory endothelium. (**a**) Exposure to TNF α activates the NF-kB signalling pathway in endothelial cells. (**b**) NF-kB-p65 translocates to the nucleus and upregulates its target genes, including Jag1. (**c**) Jag1 engages with Notch1 in adjacent cells, resulting in N1ICD release from the cell membrane. (**d**) N1ICD binds to IKK α, promoting NF-kB-p50/p65 translocation to or retention in the nucleus. (**e**) N1ICD binding to RBPJ in the nucleus activates Notch target genes, including Jag1. (**f**) NF-kB-p65 interacts with N1ICD-RBPJ to activate a subset of Notch-dependent NF-kB target genes, including Jag1, generating a positive feedback loop between Notch and NF-kB signalling.

References

1. Cines DB, Pollak ES, Buck CA, Loscalzo J, Zimmerman GA, McEver RP, Pober JS, Wick TM, Konkle BA, Schwartz BS, Barnathan ES, McCrae KR, Hug BA, Schmidt AM, Stern DM. Endothelial cells in physiology and in the pathophysiology of vascular disorders. *Blood* 1998;**91**:3527-3561.
2. Deanfield JE, Halcox JP, Rabelink TJ. Endothelial function and dysfunction: testing and clinical relevance. *Circulation* 2007;**115**:1285-1295.
3. Rajendran P, Rengarajan T, Thangavel J, Nishigaki Y, Sakthisekaran D, Sethi G, Nishigaki I. The vascular endothelium and human diseases. *International journal of biological sciences* 2013;**9**:1057-1069.
4. Pober JS. Endothelial activation: intracellular signaling pathways. *Arthritis Res* 2002;**4 Suppl 3**:S109-116.
5. Rao RM, Yang L, Garcia-Cardena G, Luscinskas FW. Endothelial-dependent mechanisms of leukocyte recruitment to the vascular wall. *Circ Res* 2007;**101**:234-247.
6. Weber C, Noels H. Atherosclerosis: current pathogenesis and therapeutic options. *Nat Med* 2011;**17**:1410-1422.
7. Artavanis-Tsakonas S, Rand MD, Lake RJ. Notch signaling: cell fate control and signal integration in development. *Science* 1999;**284**:770-776.
8. Kopan R, Ilagan MX. The canonical Notch signaling pathway: unfolding the activation mechanism. *Cell* 2009;**137**:216-233.
9. Borggrefe T, Oswald F. The Notch signaling pathway: transcriptional regulation at Notch target genes. *Cell Mol Life Sci* 2009;**66**:1631-1646.
10. Hofmann JJ, Iruela-Arispe ML. Notch signaling in blood vessels: who is talking to whom about what? *Circ Res* 2007;**100**:1556-1568.
11. Gridley T. Notch signaling in the vasculature. *Curr Top Dev Biol* 2010;**92**:277-309.
12. Nielsen CM, Cuervo H, Ding VW, Kong Y, Huang EJ, Wang RA. Deletion of Rbpj from postnatal endothelium leads to abnormal arteriovenous shunting in mice. *Development* 2014;**141**:3782-3792.
13. Morrow D, Guha S, Sweeney C, Birney Y, Walshe T, O'Brien C, Walls D, Redmond EM, Cahill PA. Notch and vascular smooth muscle cell phenotype. *Circ Res* 2008;**103**:1370-1382.
14. Lindner V, Booth C, Prudovsky I, Small D, Maciag T, Liaw L. Members of the Jagged/Notch gene families are expressed in injured arteries and regulate cell phenotype via alterations in cell matrix and cell-cell interaction. *Am J Pathol* 2001;**159**:875-883.
15. Redmond EM, Liu W, Hamm K, Hatch E, Cahill PA, Morrow D. Perivascular delivery of Notch 1 siRNA inhibits injury-induced arterial remodeling. *PLoS One* 2014;**9**:e84122.
16. Limbourg A, Ploom M, Elligsen D, Sorensen I, Ziegelhoeffer T, Gossler A, Drexler H, Limbourg FP. Notch ligand Delta-like 1 is essential for postnatal arteriogenesis. *Circ Res* 2007;**100**:363-371.
17. Wu X, Zou Y, Zhou Q, Huang L, Gong H, Sun A, Tateno K, Katsube K, Radtke F, Ge J, Minamino T, Komuro I. Role of Jagged1 in arterial lesions after vascular injury. *Arterioscler Thromb Vasc Biol* 2011;**31**:2000-2006.
18. Li Y, Takeshita K, Liu PY, Satoh M, Oyama N, Mukai Y, Chin MT, Krebs L, Kotlikoff MI, Radtke F, Gridley T, Liao JK. Smooth muscle Notch1 mediates neointimal formation after vascular injury. *Circulation* 2009;**119**:2686-2692.
19. Li D, Mehta JL. Oxidized LDL, a critical factor in atherogenesis. *Cardiovasc Res* 2005;**68**:353-354.
20. Oka C, Nakano T, Wakeham A, de la Pompa JL, Mori C, Sakai T, Okazaki S, Kawaichi M, Shiota K, Mak TW, Honjo T. Disruption of the mouse RBP-J kappa gene results in early embryonic death. *Development* 1995;**121**:3291-3301.
21. Nakashima Y, Plump AS, Raines EW, Breslow JL, Ross R. ApoE-deficient mice develop lesions of all phases of atherosclerosis throughout the arterial tree. *Arterioscler Thromb* 1994;**14**:133-140.
22. Luna-Zurita L, Prados B, Grego-Bessa J, Luxan G, del Monte G, Benguria A, Adams RH, Perez-Pomares JM, de la Pompa JL. Integration of a Notch-dependent mesenchymal gene program and

Bmp2-driven cell invasiveness regulates murine cardiac valve formation. *J Clin Invest* 2010;**120**:3493-3507.
23. Han H, Tanigaki K, Yamamoto N, Kuroda K, Yoshimoto M, Nakahata T, Ikuta K, Honjo T. Inducible gene knockout of transcription factor recombination signal binding protein-J reveals its essential role in T versus B lineage decision. *Int Immunol* 2002;**14**:637-645.
24. Gareus R, Kotsaki E, Xanthoulea S, van der Made I, Gijbels MJ, Kardakaris R, Polykratis A, Kollias G, de Winther MP, Pasparakis M. Endothelial cell-specific NF-kappaB inhibition protects mice from atherosclerosis. *Cell Metab* 2008;**8**:372-383.
25. van Vlijmen BJ, van den Maagdenberg AM, Gijbels MJ, van der Boom H, HogenEsch H, Frants RR, Hofker MH, Havekes LM. Diet-induced hyperlipoproteinemia and atherosclerosis in apolipoprotein E3-Leiden transgenic mice. *J Clin Invest* 1994;**93**:1403-1410.
26. Chevre R, Gonzalez-Granado JM, Megens RT, Sreeramkumar V, Silvestre-Roig C, Molina-Sanchez P, Weber C, Soehnlein O, Hidalgo A, Andres V. High-resolution imaging of intravascular atherogenic inflammation in live mice. *Circ Res* 2014;**114**:770-779.
27. Timmerman LA, Grego-Bessa J, Raya A, Bertran E, Perez-Pomares JM, Diez J, Aranda S, Palomo S, McCormick F, Izpisua-Belmonte JC, de la Pompa JL. Notch promotes epithelial-mesenchymal transition during cardiac development and oncogenic transformation. *Genes Dev* 2004;**18**:99-115.
28. Mallat Z, Gojova A, Marchiol-Fournigault C, Esposito B, Kamate C, Merval R, Fradelizi D, Tedgui A. Inhibition of transforming growth factor-beta signaling accelerates atherosclerosis and induces an unstable plaque phenotype in mice. *Circ Res* 2001;**89**:930-934.
29. Fuster JJ, Fernandez P, Gonzalez-Navarro H, Silvestre C, Nabah YN, Andres V. Control of cell proliferation in atherosclerosis: insights from animal models and human studies. *Cardiovasc Res* 2010;**86**:254-264.
30. Hayden MS, Ghosh S. NF-kappaB, the first quarter-century: remarkable progress and outstanding questions. *Genes Dev* 2012;**26**:203-234.
31. Espinosa L, Santos S, Ingles-Esteve J, Munoz-Canoves P, Bigas A. p65-NFkappaB synergizes with Notch to activate transcription by triggering cytoplasmic translocation of the nuclear receptor corepressor N-CoR. *J Cell Sci* 2002;**115**:1295-1303.
32. Luo J, Zhou H, Wang F, Xia X, Sun Q, Wang R, Cheng B. The hepatitis B virus X protein downregulates NF-kappaB signaling pathways through decreasing the Notch signaling pathway in HBx-transformed L02 cells. *Int J Oncol* 2013;**42**:1636-1643.
33. Shin HM, Minter LM, Cho OH, Gottipati S, Fauq AH, Golde TE, Sonenshein GE, Osborne BA. Notch1 augments NF-kappaB activity by facilitating its nuclear retention. *Embo J* 2006;**25**:129-138.
34. Song LL, Peng Y, Yun J, Rizzo P, Chaturvedi V, Weijzen S, Kast WM, Stone PJ, Santos L, Loredo A, Lendahl U, Sonenshein G, Osborne B, Qin JZ, Pannuti A, Nickoloff BJ, Miele L. Notch-1 associates with IKKalpha and regulates IKK activity in cervical cancer cells. *Oncogene* 2008;**27**:5833-5844.
35. Vilimas T, Mascarenhas J, Palomero T, Mandal M, Buonamici S, Meng F, Thompson B, Spaulding C, Macaroun S, Alegre ML, Kee BL, Ferrando A, Miele L, Aifantis I. Targeting the NF-kappaB signaling pathway in Notch1-induced T-cell leukemia. *Nat Med* 2007;**13**:70-77.
36. Zeng Q, Jin C, Ao L, Cleveland JC, Jr., Song R, Xu D, Fullerton DA, Meng X. Cross-talk between the Toll-like receptor 4 and Notch1 pathways augments the inflammatory response in the interstitial cells of stenotic human aortic valves. *Circulation* 2012;**126**:S222-230.
37. Munch J, Gonzalez-Rajal A, de la Pompa JL. Notch regulates blastema proliferation and prevents differentiation during adult zebrafish fin regeneration. *Development* 2013;**140**:1402-1411.
38. Liu ZJ, Tan Y, Beecham GW, Seo DM, Tian R, Li Y, Vazquez-Padron RI, Pericak-Vance M, Vance JM, Goldschmidt-Clermont PJ, Livingstone AS, Velazquez OC. Notch activation induces endothelial cell senescence and pro-inflammatory response: implication of Notch signaling in atherosclerosis. *Atherosclerosis* 2012;**225**:296-303.
39. Quillard T, Charreau B. Impact of notch signaling on inflammatory responses in cardiovascular disorders. *International journal of molecular sciences* 2013;**14**:6863-6888.
40. Rizzo P, Miele L, Ferrari R. The Notch pathway: a crossroad between the life and death of the endothelium. *Eur Heart J* 2013;**34**:2504-2509.

41. Briot A, Civelek M, Seki A, Hoi K, Mack JJ, Lee SD, Kim J, Hong C, Yu J, Fishbein GA, Vakili L, Fogelman AM, Fishbein MC, Lusis AJ, Tontonoz P, Navab M, Berliner JA, Iruela-Arispe ML. Endothelial NOTCH1 is suppressed by circulating lipids and antagonizes inflammation during atherosclerosis. *J Exp Med* 2015;**212**:2147-2163.
42. Calkin AC, Lee SD, Kim J, Van Stijn CM, Wu XH, Lusis AJ, Hong C, Tangirala RI, Tontonoz P. Transgenic expression of dominant-active IDOL in liver causes diet-induced hypercholesterolemia and atherosclerosis in mice. *Circ Res* 2014;**115**:442-449.
43. Galis ZS, Khatri JJ. Matrix metalloproteinases in vascular remodeling and atherogenesis: the good, the bad, and the ugly. *Circ Res* 2002;**90**:251-262.
44. Zernecke A, Weber C. Chemokines in the vascular inflammatory response of atherosclerosis. *Cardiovasc Res* 2010;**86**:192-201.
45. Ait-Oufella H, Taleb S, Mallat Z, Tedgui A. Recent advances on the role of cytokines in atherosclerosis. *Arterioscler Thromb Vasc Biol* 2011;**31**:969-979.
46. Cole JE, Kassiteridi C, Monaco C. Toll-like receptors in atherosclerosis: a 'Pandora's box' of advances and controversies. *Trends Pharmacol Sci* 2013;**34**:629-636.
47. Ghosh S, Hayden MS. New regulators of NF-kappaB in inflammation. *Nat Rev Immunol* 2008;**8**:837-848.
48. Lawrence T. The nuclear factor NF-kappaB pathway in inflammation. *Cold Spring Harbor perspectives in biology* 2009;**1**:a001651.
49. Kanters E, Gijbels MJ, van der Made I, Vergouwe MN, Heeringa P, Kraal G, Hofker MH, de Winther MP. Hematopoietic NF-kappaB1 deficiency results in small atherosclerotic lesions with an inflammatory phenotype. *Blood* 2004;**103**:934-940.
50. Osipo C, Golde TE, Osborne BA, Miele LA. Off the beaten pathway: the complex cross talk between Notch and NF-kappaB. *Lab Invest* 2008;**88**:11-17.
51. Boonyatecha N, Sangphech N, Wongchana W, Kueanjinda P, Palaga T. Involvement of Notch signaling pathway in regulating IL-12 expression via c-Rel in activated macrophages. *Molecular immunology* 2012;**51**:255-262.
52. Wongchana W, Palaga T. Direct regulation of interleukin-6 expression by Notch signaling in macrophages. *Cell Mol Immunol* 2012;**9**:155-162.
53. Fung E, Tang SM, Canner JP, Morishige K, Arboleda-Velasquez JF, Cardoso AA, Carlesso N, Aster JC, Aikawa M. Delta-like 4 induces notch signaling in macrophages: implications for inflammation. *Circulation* 2007;**115**:2948-2956.
54. Fukuda D, Aikawa E, Swirski FK, Novobrantseva TI, Kotelianski V, Gorgun CZ, Chudnovskiy A, Yamazaki H, Croce K, Weissleder R, Aster JC, Hotamisligil GS, Yagita H, Aikawa M. Notch ligand delta-like 4 blockade attenuates atherosclerosis and metabolic disorders. *Proc Natl Acad Sci U S A* 2012;**109**:E1868-1877.
55. Zhang W, Xu W, Xiong S. Blockade of Notch1 signaling alleviates murine lupus via blunting macrophage activation and M2b polarization. *J Immunol* 2010;**184**:6465-6478.
56. Monsalve E, Ruiz-Garcia A, Baladron V, Ruiz-Hidalgo MJ, Sanchez-Solana B, Rivero S, Garcia-Ramirez JJ, Rubio A, Laborda J, Diaz-Guerra MJ. Notch1 upregulates LPS-induced macrophage activation by increasing NF-kappaB activity. *Eur J Immunol* 2009;**39**:2556-2570.
57. Aifantis I, Vilimas T, Buonamici S. Notches, NFkappaBs and the making of T cell leukemia. *Cell Cycle* 2007;**6**:403-406.
58. Bash J, Zong WX, Banga S, Rivera A, Ballard DW, Ron Y, Gelinas C. Rel/NF-kappaB can trigger the Notch signaling pathway by inducing the expression of Jagged1, a ligand for Notch receptors. *EMBO J* 1999;**18**:2803-2811.
59. Johnston DA, Dong B, Hughes CC. TNF induction of jagged-1 in endothelial cells is NFkappaB-dependent. *Gene* 2009;**435**:36-44.
60. Foldi J, Chung AY, Xu H, Zhu J, Outtz HH, Kitajewski J, Li Y, Hu X, Ivashkiv LB. Autoamplification of Notch signaling in macrophages by TLR-induced and RBP-J-dependent induction of Jagged1. *J Immunol* 2010;**185**:5023-5031.
61. Hu X, Chung AY, Wu I, Foldi J, Chen J, Ji JD, Tateya T, Kang YJ, Han J, Gessler M, Kageyama R, Ivashkiv LB. Integrated regulation of Toll-like receptor responses by Notch and interferon-gamma pathways. *Immunity* 2008;**29**:691-703.
62. Ma Y, Malbon CC, Williams DL, Thorngate FE. Altered gene expression in early atherosclerosis is blocked by low level apolipoprotein E. *PLoS One* 2008;**3**:e2503.

63. Bonetti PO, Lerman LO, Lerman A. Endothelial dysfunction: a marker of atherosclerotic risk. *Arterioscler Thromb Vasc Biol* 2003;**23**:168-175.
64. Davignon J, Ganz P. Role of endothelial dysfunction in atherosclerosis. *Circulation* 2004;**109**:III27-32.
65. Martin BJ, Anderson TJ. Risk prediction in cardiovascular disease: the prognostic significance of endothelial dysfunction. *Can J Cardiol* 2009;**25 Suppl A**:15A-20A.

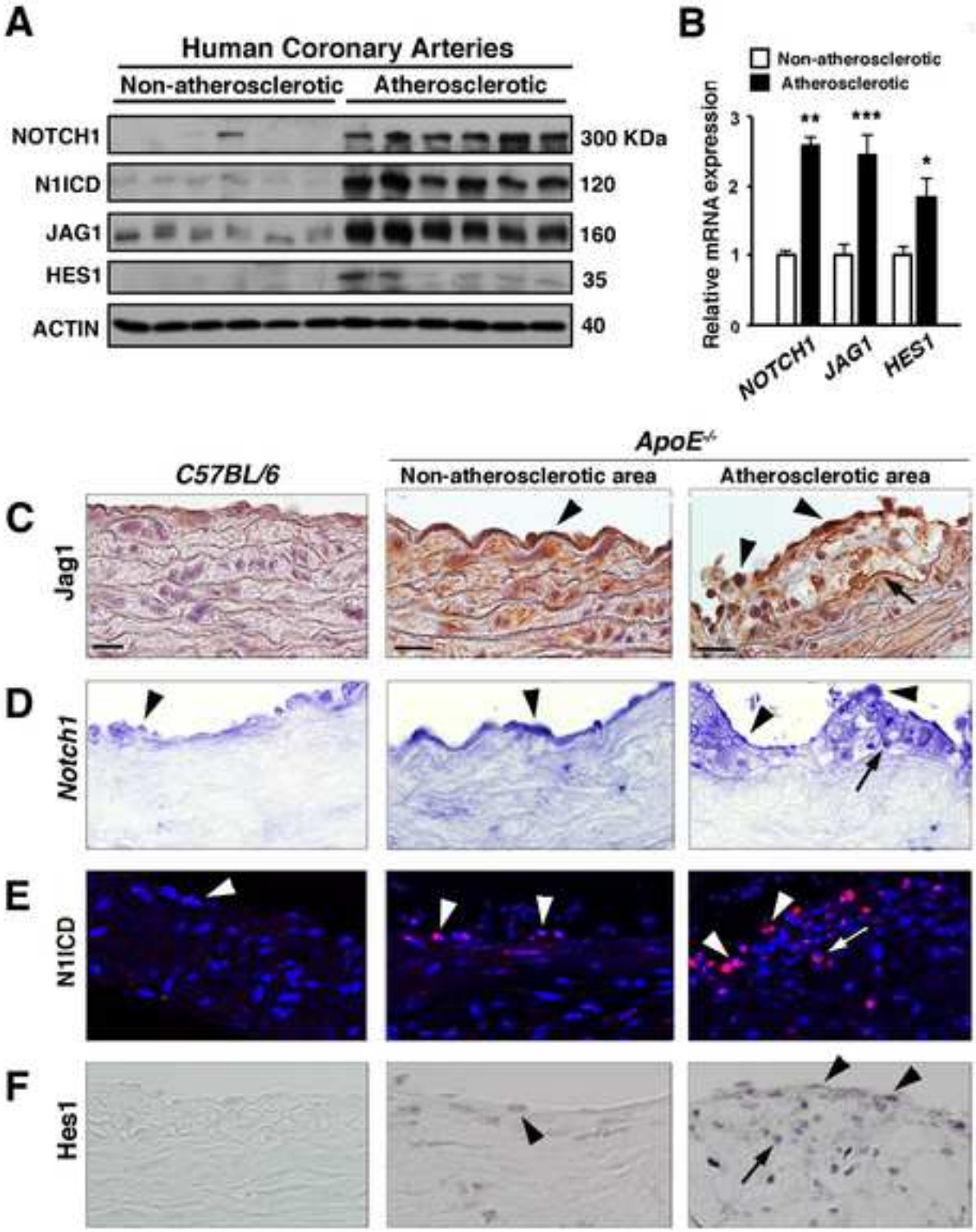

Figure 1_Nus, Martínez-Poveda, MacGrogan et al.

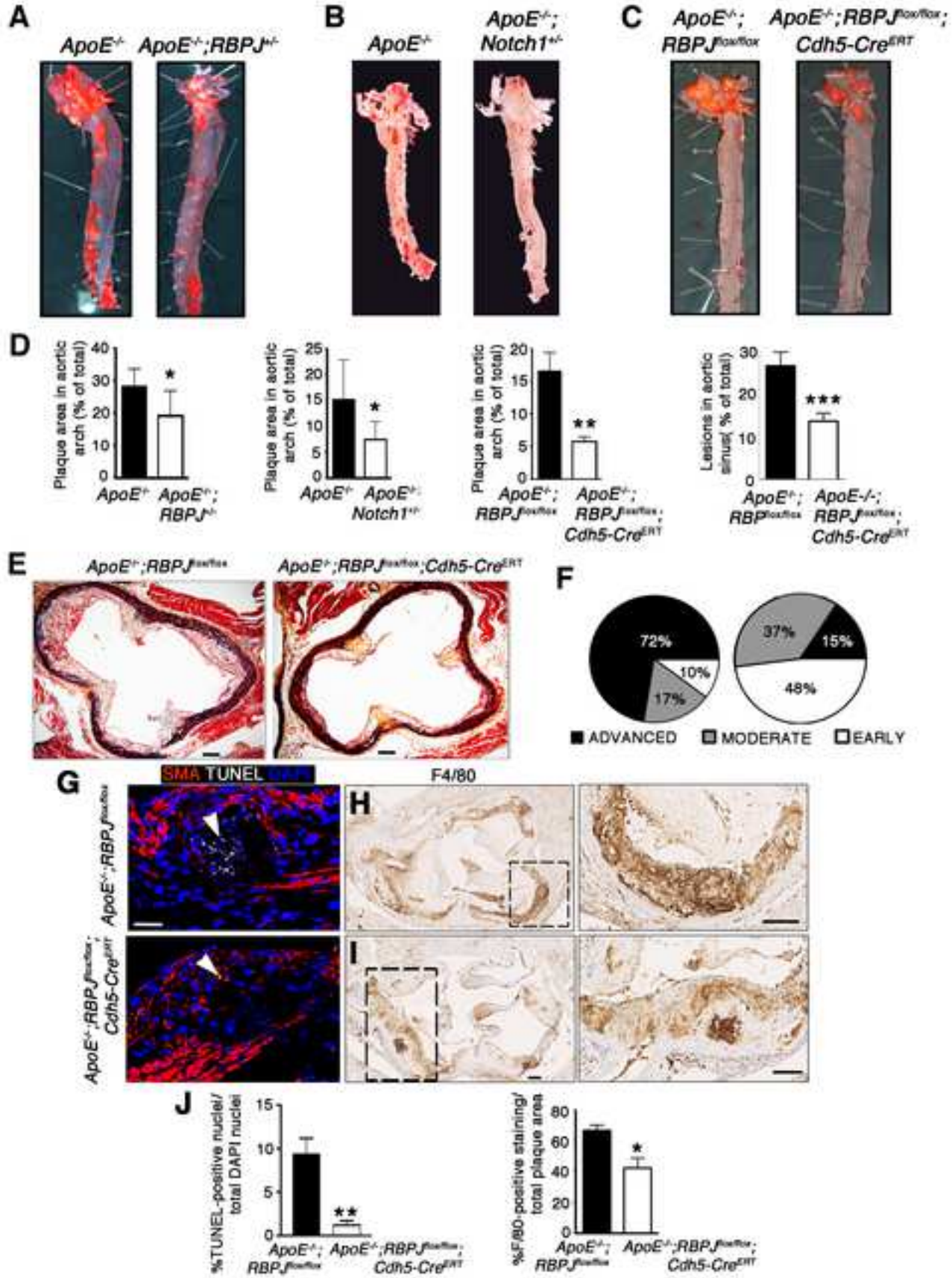

Figure 2_Nus, Martínez-Poveda, MacGrogan et al.

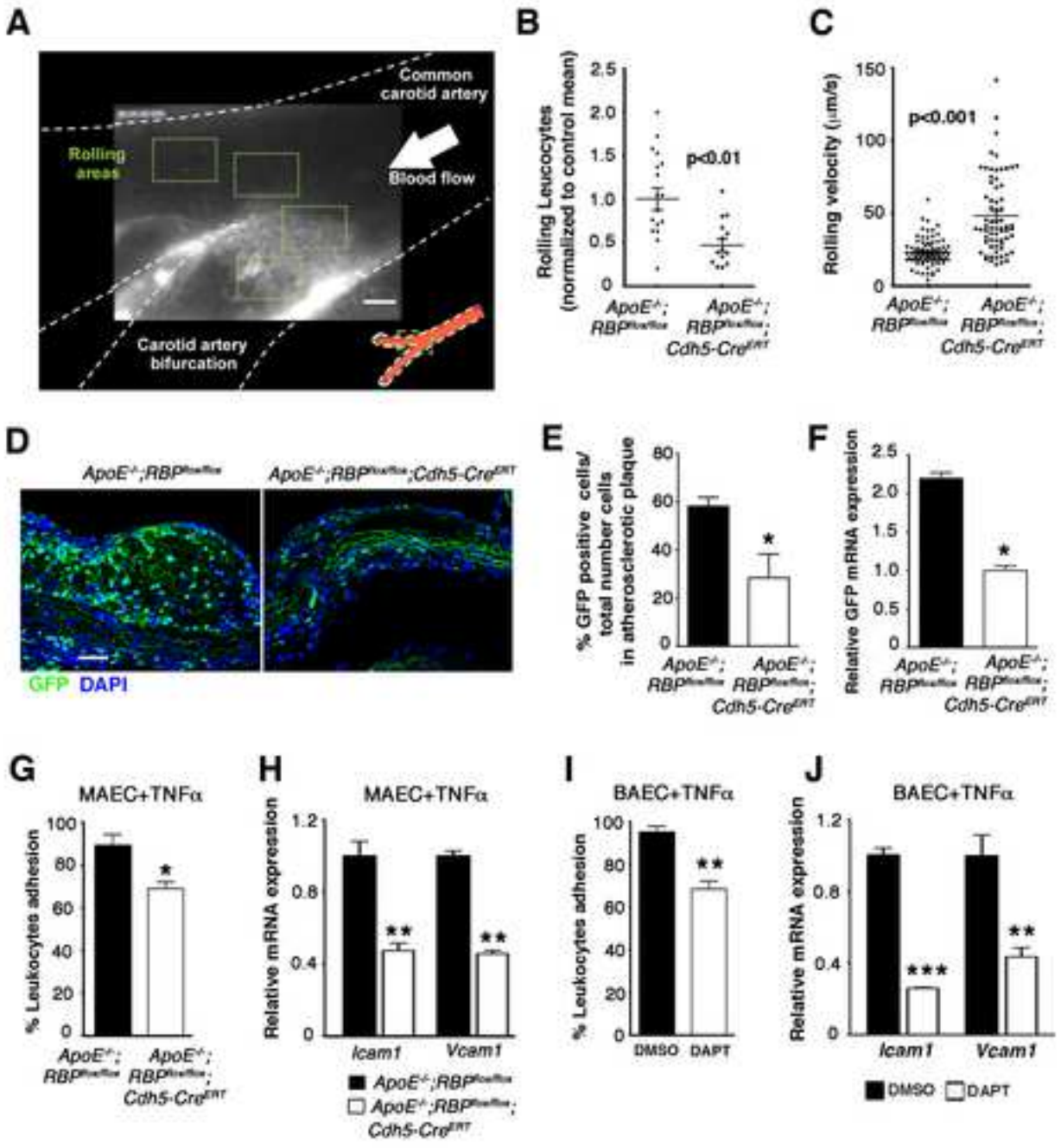

Figure 3_Nus, Martínez-Poveda, MacGrogan et al.

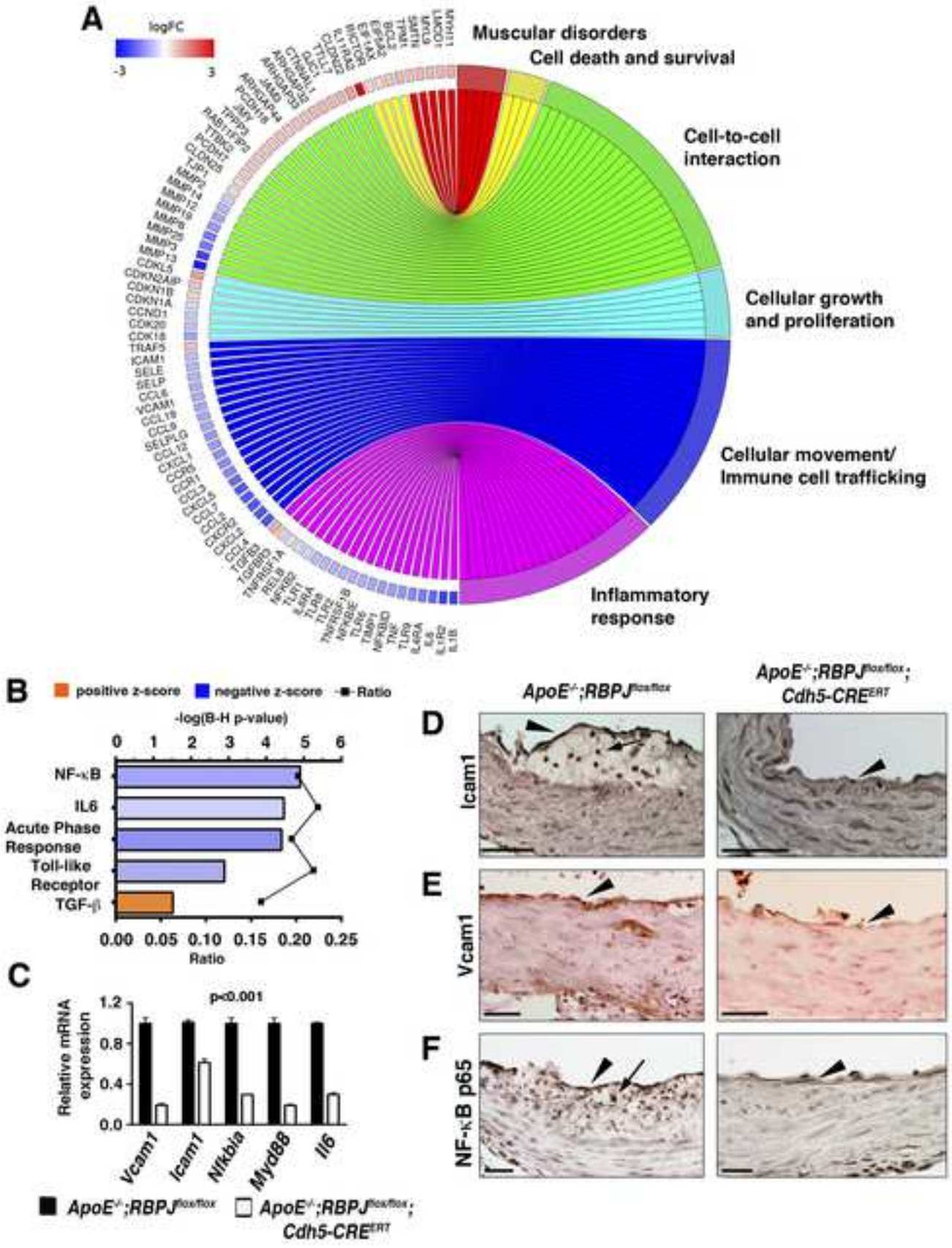

Figure 4_Nus, Martinez-Poveda, MacGrogan et al

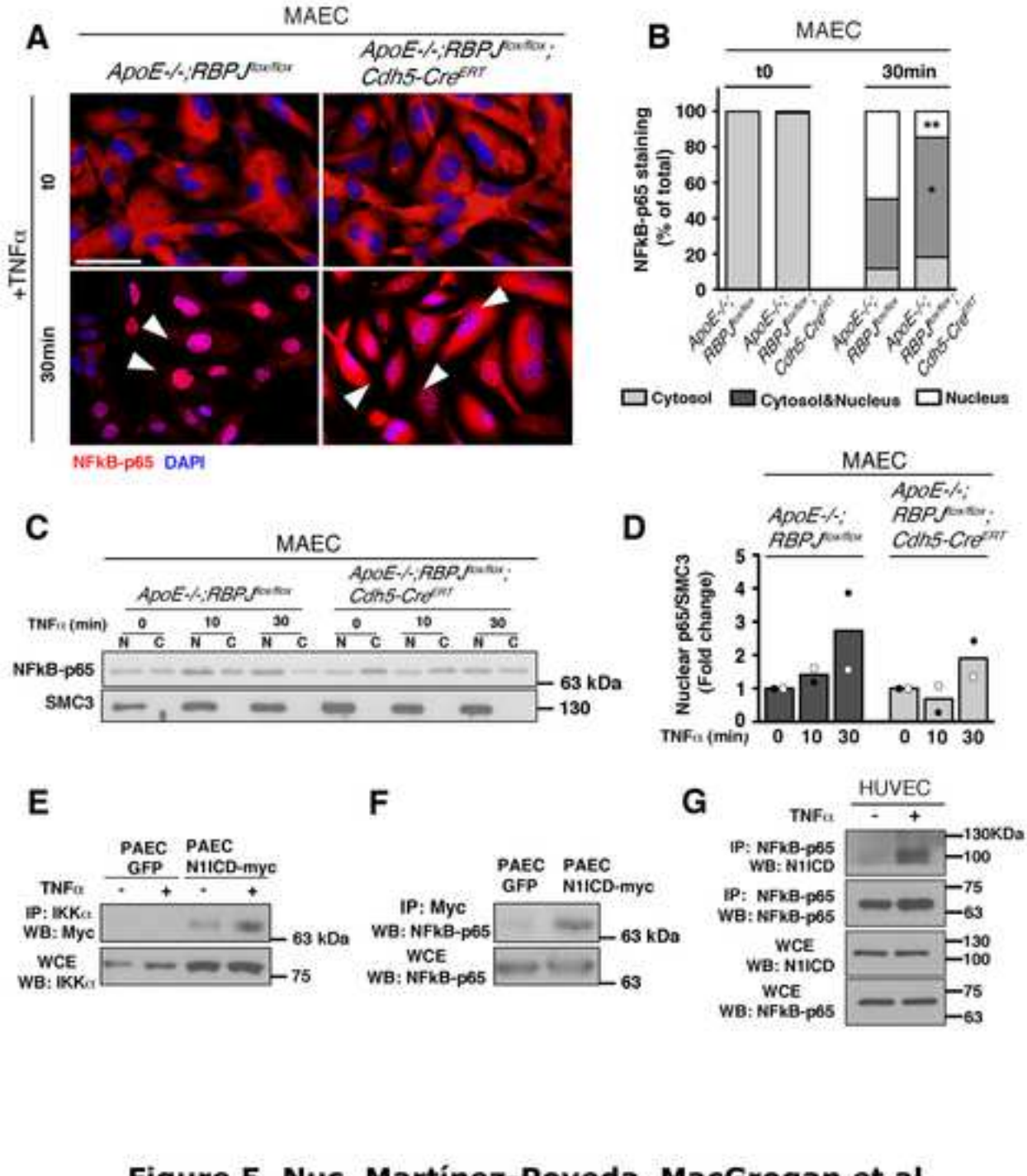

Figure 5_Nus, Martínez-Poveda, MacGrogan et al.

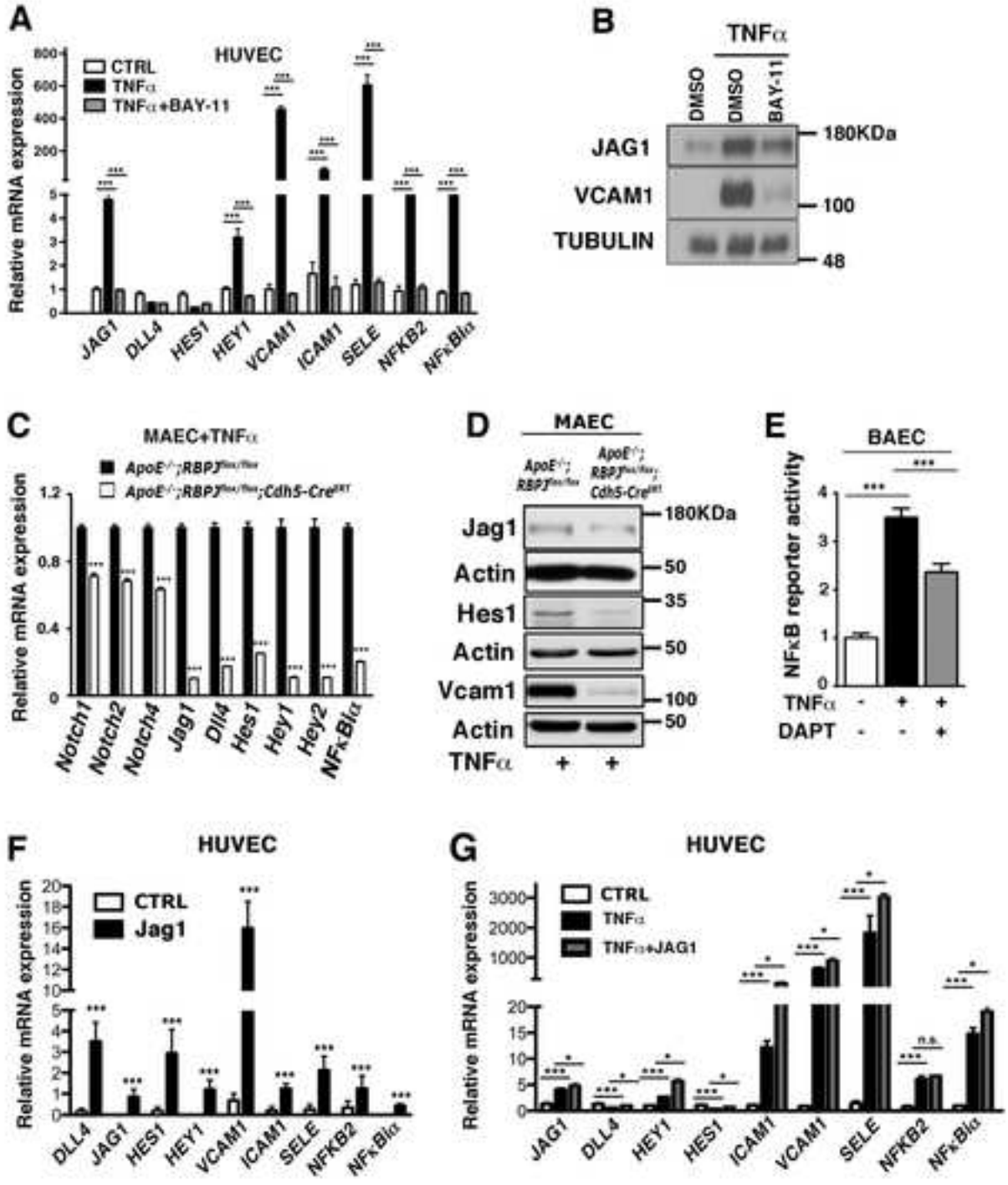

Figure 6_Nus, Martínez-Poveda, MacGrogan et al.

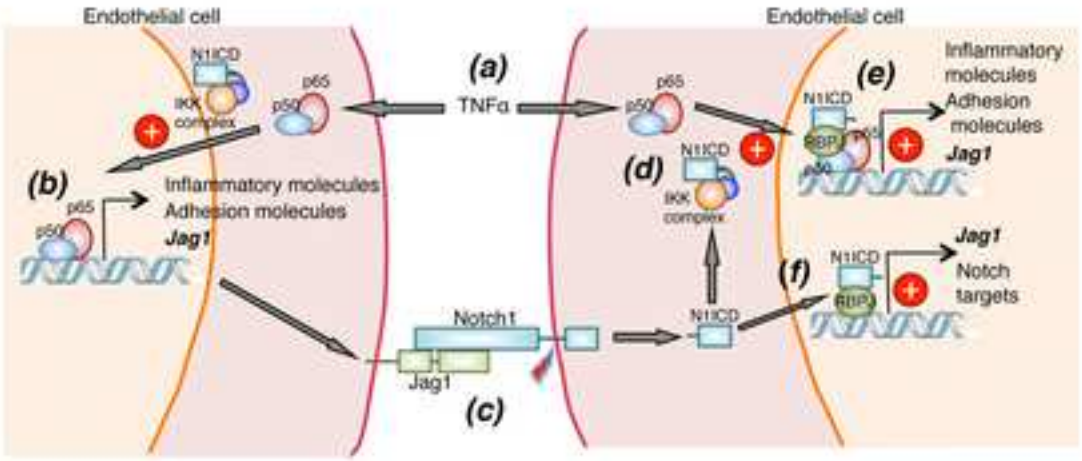

Figure 7_Nus, Martínez-Poveda, MacGrogan et al.